Published OnlineFirst November 3, 2009; DOI: 10.1158/1541-7786.MCR-09-0069

The Alkylphospholipid Perifosine Induces Apoptosis and p21-Mediated Cell Cycle Arrest in Medulloblastoma

Anil Kumar, Helen L. Fillmore, Renu Kadian, William C. Broaddus, Gary W. Tye, and Timothy E. Van Meter

Department of Neurosurgery and Harold F. Young Neurosurgical Center, Virginia Commonwealth University, School of Medicine, Richmond, Virginia

Abstract

Medulloblastoma is the most common malignant cancer of the central nervous system in children. AKT kinases are part of a survival pathway that has been found to be significantly elevated in medulloblastoma. This pathway is a point of convergence for many growth factors and controls cellular processes that are critical for tumor cell survival and proliferation. The alkyl-phospholipid perifosine [octadecyl-(1,1-dimethyl-4-piperidylio) phosphate] is a small molecule inhibitor in clinical trials in peripheral cancers which acts as a competitive inhibitor of AKT kinases. Medulloblastoma cell cultures were used to study the effects of perifosine response in preclinical studies *in vitro*. Perifosine treatment led to the rapid induction of cell death in medulloblastoma cell lines, with pronounced suppression of phosphorylated AKT in a time-dependent and concentration-dependent manner. LD_{50} concentrations were established using viability assays for perifosine, cisplatin, and etoposide. LD_{50} treatment of medulloblastoma cells with perifosine led to the cleavage of caspase 9, caspase 7, caspase 3, and poly-ADP ribosylation protein, although caspase 8 was not detectable. Combination single-dose treatment regimens of perifosine with sublethal doses of etoposide or irradiation showed a greater than additive effect in medulloblastoma cells. Lower perifosine concentrations induced cell cycle arrest at the G_1 and G_2 cell cycle checkpoints, accompanied by increased expression of the cell cycle inhibitor $p21^{cip1/waf1}$. Treatment with p21 small interfering RNA prevented perifosine-induced cell cycle arrest. These findings indicate that perifosine, either alone or in combination with other chemotherapeutic drugs, might be an effective therapeutic agent for the treatment of medulloblastoma. (Mol Cancer Res 2009;7(11):1813–21)

Introduction

Medulloblastoma is the most common and fatal brain tumor among children, accounting for 12% to 25% of all pediatric tumors of the central nervous system (1). Medulloblastomas are most commonly characterized by highly mitotic small, round cells with a high nuclear to cytoplasmic ratio, and are classified as primitive neuroectodermal tumors. The current treatment includes surgery, chemotherapy, and radiation therapy. Current clinical trials include high-dose chemotherapy for high-risk and recurrent medulloblastoma, but few targeted small molecule inhibitors specific to medulloblastoma have been described. Despite these therapies, 5-year survival is at best 60% to 70%, and moreover, these therapies affect the developing central nervous system causing memory, attention, motor function, language, and visuospatial deficits (2). There is a need for the development of novel agents that can avoid these deleterious treatment sequelae. Several signaling molecules have been associated with medulloblastoma development, including Sonic hedgehog (3) and members of the WNT pathway (4). Recently, AKT kinases, which were originally discovered as homologues to the oncogene in the thymoma-associated acute transforming retrovirus AKT-8 (5), have been found to have elevated activation levels in these tumors. Furthermore, elevated active AKT levels have been shown to be associated with features of malignancy such as proliferation, survival, glucose metabolism, and revascularization in other cancers (6, 7). Three AKT isotypes have been identified, AKT1, AKT2, and AKT3 (8). It is currently unknown which of these isotypes are predominantly expressed in medulloblastoma. In animal models, exogenous activation of the AKT1 kinase pathway significantly enhanced Sonic hedgehog–induced medulloblastoma formation (9), indicating a promalignancy interaction of these two pathways.

Due to the importance of AKT signaling in cancer biology, several small inhibitory molecules of the AKT pathway have been developed for clinical use in cancer therapy (10). As AKT activation is mediated by active upstream receptor proteins such as growth factor and adhesion receptors, and is activated largely within lipid-dependent protein signaling complexes at cell membranes, phospholipid analogue compounds known as alkylphospholipids were developed to interfere with this process, including perifosine [octadecyl-(1,1-dimethyl-4-piperidylio) phosphate].

Perifosine is a novel phospholipid analogue which is currently undergoing phase I and phase II clinical evaluations (11, 12). Although the exact mechanisms of action of perifosine are still being investigated, it is thought to interfere with the turnover and synthesis of endogenous membrane phospholipids, thereby

Received 2/20/09; revised 5/22/09; accepted 7/21/09; published OnlineFirst 11/3/09.
Grant support: Supported in part by the Cherise Fleming Translational Grant from the American Brain Tumor Association and the Andrew Christian Bryce PNET Award from the National Brain Tumor Foundation. The VCU Pediatric Neuro-Oncology Program was generously supported by the F. Norton Hord, Jr., and Michael Bergen, Jr., families, and the Medical College of Virginia Foundation.
Requests for reprints: Timothy Van Meter, Department of Neurosurgery, Virginia Commonwealth University School of Medicine, 401 North Clay Street, Box 980631 Richmond, VA 23298-0631. Phone: 804-828-2564; Fax: 804-827-1487. E-mail: tevanmet@vcu.edu

doi:10.1158/1541-7786.MCR-09-0069

Published OnlineFirst November 3, 2009; DOI: 10.1158/1541-7786.MCR-09-0069

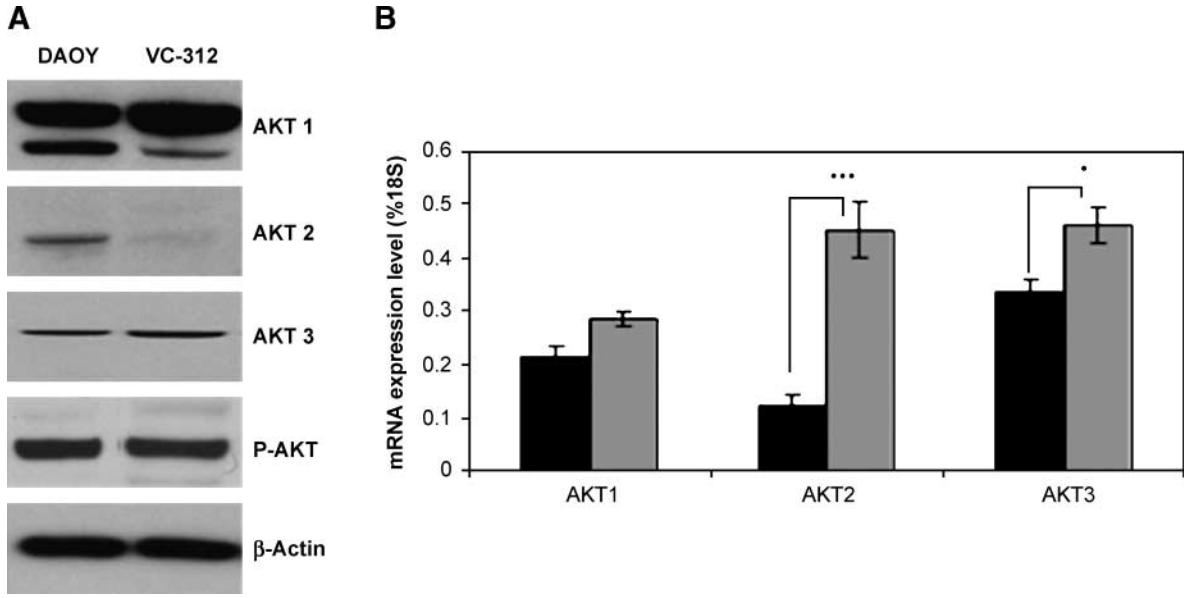

FIGURE 1. Expression of AKT isoforms in medulloblastomas. **A.** Detection of all three AKT isoforms expressed in medulloblastoma cell lines. Western blotting analysis of protein lysates derived from DAOY and VC-312 were probed with isoform-specific antibodies for Akt1, Akt2, Akt3, and P-AKT phosphorylated Ser^{473}. β-Actin is used as an internal control. **B.** TaqMan assay of AKT isoforms in medulloblastoma tissues *in vivo* compared with normal cerebellum (n = 4 normal, *black columns*; n = 11 medulloblastoma, *gray columns*; ***, P = 0.001; *, P = 0.02, t test for comparison of the mean values).

affecting lipid-mediated signal transduction pathways, including inhibition of AKT (13), mitogen-activated protein kinase activation (14), and activation of c-*Jun*-NH_2-kinase. Perifosine is an orally bioavailable drug that has shown antitumor activity in preclinical models (15, 16). Previously, perifosine has been shown to induce apoptosis and cell cycle arrest in cancer cell lines (17-19). However, perifosine has not been studied in medulloblastoma.

In this study, our data show that endogenous active AKT is present at high levels compared with normal brain samples in medulloblastoma and derivative cell lines. Treatment of these cell lines with perifosine decreases active AKT levels in a dose-dependent and time-dependent manner. We showed that perifosine treatment led to rapid decreases in cell survival in medulloblastoma cells. In an attempt to understand the mechanism of perifosine-mediated cytotoxicity, we examined the effect of perifosine on apoptotic regulatory proteins and the cell cycle distribution after treatment. Our data shows that perifosine treatment led to the upregulation of caspase activity and programmed cell death mechanisms that are consistent with the intrinsic apoptotic pathway, including cleavage of caspase 9, caspase 7, caspase 3, and poly-ADP ribosylation protein (PARP) in both cell lines and p21-mediated cell cycle arrest. We also report that exposure to etoposide and radiation followed by posttreatment with perifosine resulted in greater than additive effect cell death, indicating that perifosine has chemosensitizing and radiosensitizing effects on medulloblastoma cells. These findings indicate that perifosine, either alone or in combination with other chemotherapeutic drugs, might be an effective therapeutic agent for the treatment of medulloblastoma, the most common malignant brain cancer in children.

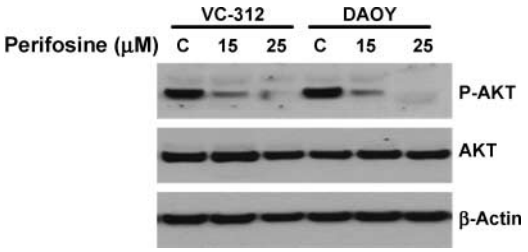

FIGURE 2. Concentration-dependent suppression of active AKT by perifosine in VC312 and DAOY cells. VC312 and DAOY cells were treated with increasing concentrations (0, 15, 25 μmol/L) of perifosine for 3 h and cell lysates were then subjected to Western blotting analysis.

Results

AKT Isotype Expression and Its Activation Level in Medulloblastoma

To characterize endogenous protein expression levels of AKT isotypes, AKT1, AKT2, AKT3, and the phosphorylated forms of AKT at the two major phosphorylation sites, Thr^{308} and Ser^{473} were examined by Western blot under normal growth conditions. As show in Fig. 1A, AKT1 and AKT3 were detected in both cell lines at significant levels, whereas AKT2 protein was detected more predominantly in DAOY cells. Despite apparent differences in isotype expression levels, robust phosphorylated AKT was detected in both cell lines using antibodies nonselective for individual isotypes. These results suggest that, even though the protein expression levels of AKT isotypes may vary in these cell lines, both have highly active endogenous AKT signaling. Transcript expression levels for each AKT isotype were also examined in medulloblastoma clinical specimens (n = 11) compared with normal cerebellum (n = 4). The abundance of mRNA was examined by TaqMan quantitative PCR assay. As shown in Fig. 1B, mRNA levels for AKT1 were similar to normal brain, whereas AKT2 and

Published OnlineFirst November 3, 2009; DOI: 10.1158/1541-7786.MCR-09-0069

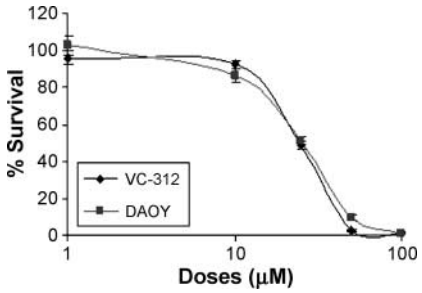

FIGURE 3. Effect of perifosine administration on medulloblastoma cell viability. Cells were seeded at a density of 10^3 cells per well in 96-well plate in replicates of six and incubated for 24 h with 1, 10, 25, 50, and 100 μmol/L perifosine. Relative cell number was measured by luminescent ATP viability assay. Bars, SD within an experiment, with significant differences determined using Student's *t* test ($P < 0.05$). Representative experiments from four independent trials.

AKT3 were significantly elevated in medulloblastomas (*t* test, ***, $P = 0.001$ and *, $P = 0.02$, respectively) measured as a ratio to the β-actin internal control mRNA.

Suppression of AKT by Perifosine in Medulloblastoma

Perifosine impairs AKT phosphorylation by interfering with the binding of the PH domain of AKT to PIP3 (8). We first examined the effect of perifosine on the phosphorylation status of AKT in medulloblastoma cell lines (Fig. 2). Western blot analysis with phosphorylation-specific AKT antibodies showed a decrease in phosphorylated AKT in a concentration-dependent manner at 3 hours. To determine the time-dependent effect of perifosine on phosphorylated active AKT levels, we treated DAOY and VC312 cells with 25 μmol/L of perifosine (the approximate LD_{50} for both cell lines). There is complete loss of detectable phosphorylated AKT in both cell lines at this concentration by 6 hours. As AKT activity depends on its phosphorylation status and perifosine treatment leads to loss of phosphorylation, this indicates that perifosine induces the inactivation of AKT in medulloblastoma cell lines.

Inhibition of AKT Decreases Cell Viability in Medulloblastoma

To determine whether perifosine treatment would result in a decrease in viability of medulloblastoma cells, DAOY and VC-312 cells were incubated in the presence of increasing concentrations of perifosine for 24 h. Cell viability was evaluated by Cell Titer-Glo luminescent ATP assay. Perifosine induced a dose-dependent decrease in cell viability in both cell lines, shown in Fig. 3. The LD_{50} (lethal dose to 50%) for DAOY and VC-312, determined using three replicate viability assays, was 25 μmol/L. Rapid loss in viability was apparent at concentrations >10 μmol/L, and near complete loss in survival was observed at 50 μmol/L.

Effect of Perifosine on Apoptotic Pathway

We further examined the induction of caspase cleavage in time course studies using concentrations at or above the established LD_{50} for perifosine. To determine the mechanism of cell death after perifosine treatment, medulloblastoma cells were treated with perifosine and examined for decreases in cellular proteins related to apoptosis. PARP and caspase cleavage have been used as sensitive indicators of cellular apoptosis. Cleavage of the effector caspases 3 and 7, and the upstream initiator caspase 9, was assayed by Western blotting using antibodies which detect procaspases and cleavage-specific forms indicative of activity. Treatment of DAOY and VC-312 cells with 25 and 40 μmol/L doses of perifosine, respectively, resulted in a time-dependent cleavage of caspase 9 (35 kDa), caspase 3 (17/19 kDa), caspase 7 (20 kDa), and PARP (85 kDa), shown in Fig. 4. We were unable to detect caspase 8 in either cell line (data not shown). As shown in Fig. 4B and C, caspase 3 and PARP cleavage were detected by 6 hours in both cell lines, concurrent with loss of detectable phosphorylated AKT (Fig. 4A). No significant change in total AKT was observed under the same conditions. Caspases 9 and 7 were also present in cleaved forms by 6 hours (total and cleaved forms shown for DAOY in Fig. 4D). Repeated viability assays incorporating peptide and small molecule caspase 3 inhibitors were done to further validate the role of apoptosis in medulloblastoma cell death after perifosine. Preincubation with caspase 3 inhibitors led to dose-dependent reversal of perifosine-induced cell death, further implicating caspase-mediated apoptotic cell death in the perifosine response in medulloblastoma cells (Fig. 4E).

Perifosine Sensitizes Medulloblastoma Cells to Etoposide and Radiation-Induced Cytotoxicity

We next examined whether inhibition of the AKT survival pathway enhances chemotherapy-induced or radiation-induced cytotoxicity. The combined effect of perifosine with commonly administered chemotherapy drugs etoposide and cisplatin, or with ionizing radiation, was evaluated in dose-response studies. Figure 5 shows the dose-dependent effects of etoposide in DAOY and VC312 cell. LD_{20} doses were first chosen to evaluate the combined effects of perifosine on cell viability. The effects of perifosine were additive in both cell lines (data not shown). In contrast, low doses of etoposide with clinically achievable concentrations of perifosine (10 μmol/L) generated greater than additive losses in cell survival in DAOY cells (Fig. 5A). Comparison of mean cell survival values using a *t* test approach showed significant differences between etoposide treatment alone and in combination with perifosine ($P = 0.0002$ for 0.1 μmol/L etoposide and $P = 0.0000007$ in combination with 10 or 20 μmol/L perifosine) and versus VC312 and DAOY, respectively. Dose-dependent cell survival studies with single-dose ionizing radiation showed LD_{50} values of 10 Gy for DAOY cells and for VC312 cells (data not shown). LD_{10} values were used in combination treatments with increasing concentrations of perifosine (10-30 μmol/L). As shown in Fig. 5B, 8 Gy treatment of DAOY cells and 10 μmol/L of perifosine caused a significant increase in cell killing compared with either treatment alone ($P = 0.0032$ and 0.0013 for combination treatment with 8 Gy single dose and 10 or 20 μmol/L perifosine, respectively). Combination index (CI) values were used to describe combined drug effect. Synergistic effect is considered when $CI < 0.85$ and antagonistic when $CI > 1.1$ and additive when values are close to 1. CI values calculated under optimized conditions for DAOY were determined to be 0.84126 for DAOY treated 72 h with 0.1 μmol/L etoposide and 10 μmol/L perifosine, and 0.783 for VC312 cells under the same conditions. Similarly, after 8 Gy irradiation, the CI values for

Published OnlineFirst November 3, 2009; DOI: 10.1158/1541-7786.MCR-09-0069

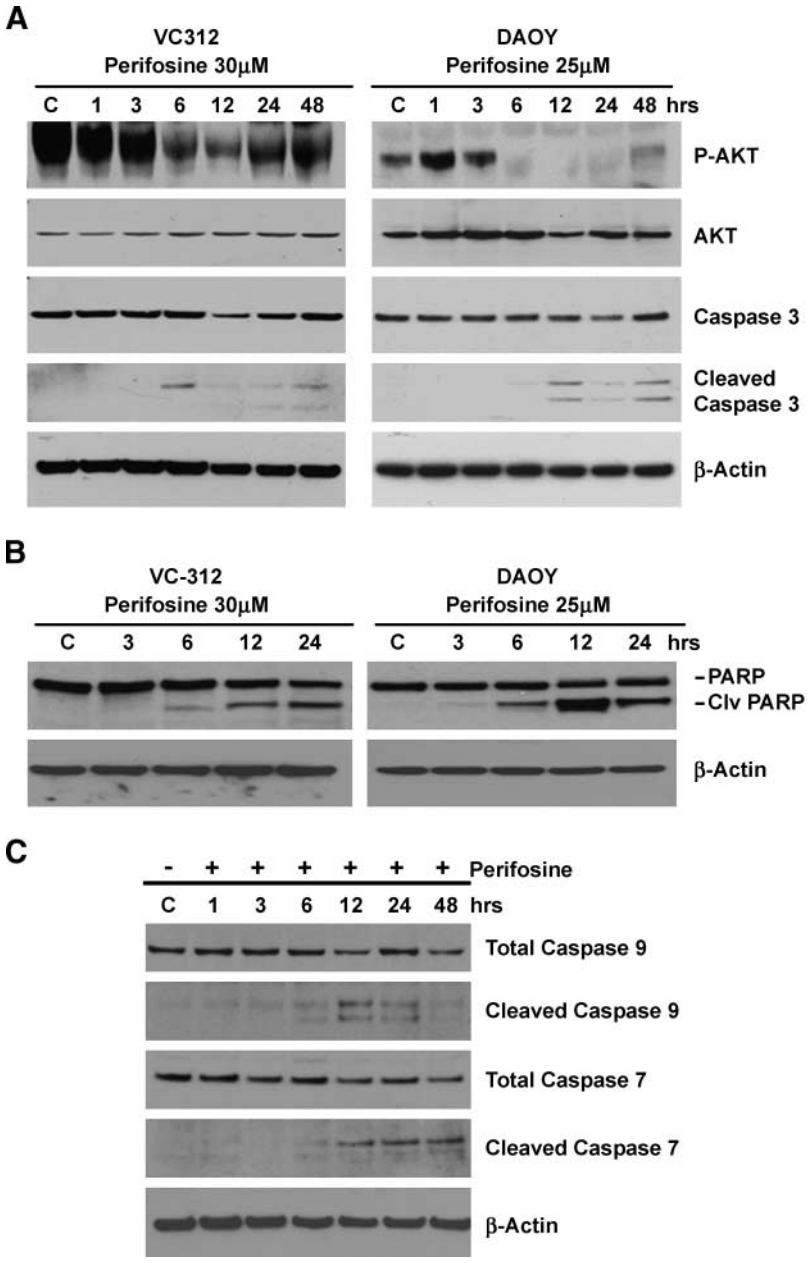

FIGURE 4. Time-dependent effect of perifosine on apoptotic induction. **A.** The effect of perifosine on phosphorylated AKT, total AKT, and caspase 3 cleavage in DAOY and VC-312 cells. **B.** PARP cleavage detected in DAOY and VC-312 after perifosine. **C.** The effect of perifosine on caspase 9 and caspase 7 cleavage in DAOY and VC-312 cells. DAOY and VC-312 cells were treated with 25 and 30 μmol/L of perifosine, respectively, and cell lysates were then subjected to Western blotting.

combined treatment with 10 μmol/L were 0.73 for DAOY, and 1.1 for VC312, indicating synergy in DAOY, but not in VC312 at the doses examined.

Effect of Perifosine on the Cell Cycle in Medulloblastoma Cells

To examine mechanisms other than caspase-mediated apoptosis responsible for the cytotoxic effects of perifosine, and because of the reported link of AKT activity with the cell cycle in medulloblastoma and other cancers, we sought to investigate the effect of perifosine on DAOY and VC-312 cell proliferation. To determine the dose-dependent effect, DAOY and VC-312 cells were exposed to increasing concentrations of perifosine (5-30 μmol/L) for 12 and 24 hours and then analyzed for cell cycle profiles by determining the DNA content of treated cell populations (Fig. 6). Minimal effects were seen in cell cycles at the 5 μmol/L dose of perifosine in DAOY and VC-312. The maximum effect was seen at the 15 μmol/L dose of perifosine, in which there was a significant increase in the G_2-M phase population (paired t test, $P = 0.00039$) and decrease in G_0-G_1 and S phase ($P = 0.00038$ and 0.017, respectively) of DNA in VC-312 cells (Fig. 6B). In contrast to VC-312, perifosine treatment led to a significant increase in G_0-G_1 (0.00117) and decrease in G_2-M ($P = 0.0134$) phases in DAOY cells (Fig. 6C). Further examination of the time-dependency of the observed growth arrest determined that there was a more significant difference at 24 hours as compared with 12 hours, consistent with an accumulation of treated cells at a cell cycle checkpoint.

Published OnlineFirst November 3, 2009; DOI: 10.1158/1541-7786.MCR-09-0069

Dependence of Perifosine-Induced Cell Cycle Arrest on p21WAF1

To determine which cell cycle regulatory proteins were involved in the observed cell cycle arrest following perifosine treatment, Western blotting analysis of control and treated cell lysates was done. No change was observed in cdc-2 or Rb phosphorylation levels, or of p53, p16, or MDM-2 expression levels. In contrast, the p21WAF1 cyclin-dependent kinase inhibitor protein level was found to be robustly increased by perifosine in a dose-dependent manner within 6 hours of treatment. Figure 7 shows the increase in p21 protein levels after 24 hours of perifosine treatment in two medulloblastoma cell lines, without an overall change in p53 levels (DAOY), or even a decrease in p53 (VC312). This data argues against a role for p53 in p21 induction via transcriptional upregulation of the p21WAF1 promoter, particularly because DAOY cells bear mutant p53. To further investigate the role of p21WAF1 in perifosine-induced cell cycle arrest, small interfering RNA (siRNA) duplexes were transfected into the two cell lines to knock out p21 protein expression prior to perifosine treatment. After successful knockdown of p21WAF1, as shown by Western blotting in Fig. 8A, flow cytometric analyses were repeated to analyze cell cycle distribution. Loss of p21WAF1 by RNA interference prevented the perifosine-induced cell cycle arrest, whereas perifosine induced arrest at cell cycle checkpoints in nontransfected controls and nontargeting siRNA control cell populations (Fig. 8B).

Discussion

Medulloblastomas are the most common malignant pediatric brain tumors, but their molecular pathology is not fully understood. The phosphatidylinositol 3′-kinase (PI3K)–mediated AKT signaling pathway has been found to have a role in tumor cell survival and proliferation (20). Recently, elevated activation of the PI3K/AKT signaling pathway has been found to be a common event in medulloblastomas (21). The activation of AKT signaling has been attributed due to deregulation of different components of the PI3K/AKT pathway, including PTEN deletion (22), PI3K gene amplification, AKT amplification (23), and AKT overexpression (20). The exact mechanism of AKT activation in medulloblastomas is still unknown, but one possible mechanism is reduced expression of PTEN (21). Perifosine (octadecyl-[*N*,*N*-dimethyl-piperidinio-4-yl]-phosphate), a synthetic alkyl-lysophospholipid structurally related to ether lipids, is thought to interfere with AKT-mediated signal transduction pathways after it is internalized via raft-mediated endocytosis (24). Here, we have shown the efficacy of perifosine in decreasing phosphorylated AKT in DAOY and VC-312 medulloblastoma cell lines. Perifosine, in a dose-dependent manner, decreased cell survival of both cell lines, and the loss of cell viability followed a marked reduction in phosphorylated AKT-S473. Perifosine treatment decreased phosphorylated AKT levels in both a dose-dependent and time-dependent manner. This data is in accordance with previously reported data of the action of perifosine on other cell lines (25). Perifosine treatment resulted in the upregulation of P-ERK in medulloblastoma cell lines. The upregulation of ERK signaling could be because of the activation of Raf-mediated activation of mitogen-activated signaling pathways as P-AKT has been reported to negatively regulate Raf-1 (26). The decreased cell survival in medulloblastoma was due to apoptosis and a decrease in cell cycle progression, as indicated by Western blot and flow cytometric analyses of samples treated with perifosine. Perifosine treatment resulted in the activation of multiple caspases including initiator caspase 9, and effector caspase 3 and caspase 7. Perifosine treatment also led to the cleavage of PARP, which is a caspase 3 substrate. Inhibition of caspase 3 using pharmacologic inhibitors attenuated a perifosine-induced decrease in cell viability (data not shown), substantiating the role of caspase activation in perifosine-induced cell death. Perifosine treatment has been found to induce the activation of Fas/CD95 death receptor in multiple myeloma cells, leading to caspase 8 activation, in turn, leading to the cleavage of Bid and subsequent caspase 9 activation (27, 28). Perifosine might have similar mechanisms of action in medulloblastomas. However, we were unable to detect caspase 8 expression in either cell line examined, consistent with reports of epigenetic silencing of caspase 8 in medulloblastoma.

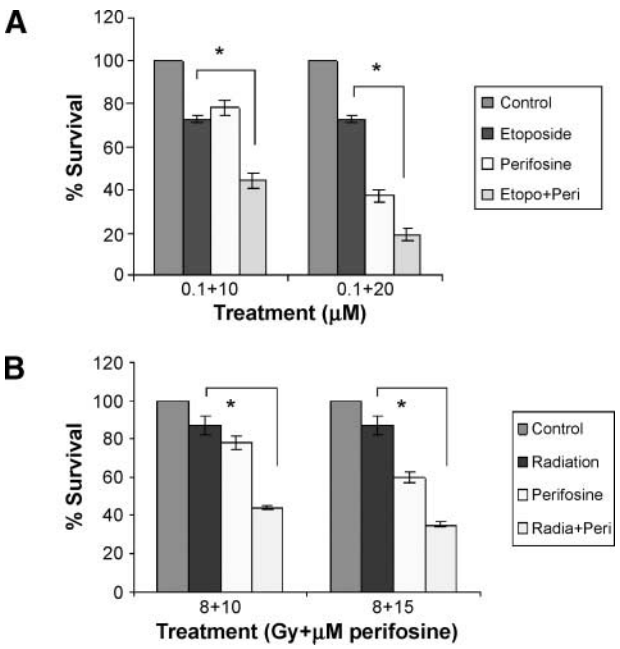

FIGURE 5. Perifosine cotreatment augments cell death by etoposide and irradiation in medulloblastoma cells. DAOY cells were exposed for 72 h to the indicated concentration of etoposide (0.1 μmol/L; **A**) and irradiation (8 Gy; **B**), as single treatments alone or in combination with 10, 15, and 20 μmol/L perifosine added after 24 h. Cell viability was evaluated by ATP viability assays. *$P < 0.05$ (see Results for respective *p*-values).

To examine the cytotoxic effect of perifosine in more detail, cell cycle progression of medulloblastoma cell lines exposed to perifosine was examined. We observed that a 15 μmol/L perifosine treatment for 24 hours led to the accumulation of DAOY cells in G_1 phase and VC-312 cells in the G_2-M phase of cell cycle. As cell cycle progression is governed by the cyclical activation of cyclin-dependent kinases, which are regulated by cyclins and cyclin-dependent kinase inhibitors (p21 and p27; ref. 29), it was of interest to evaluate the effect of perifosine on these cell cycle regulatory proteins. Unlike most chemotherapeutic anticancer drugs, which target DNA, perifosine is inserted in the plasma membrane and is thought to interfere

Published OnlineFirst November 3, 2009; DOI: 10.1158/1541-7786.MCR-09-0069

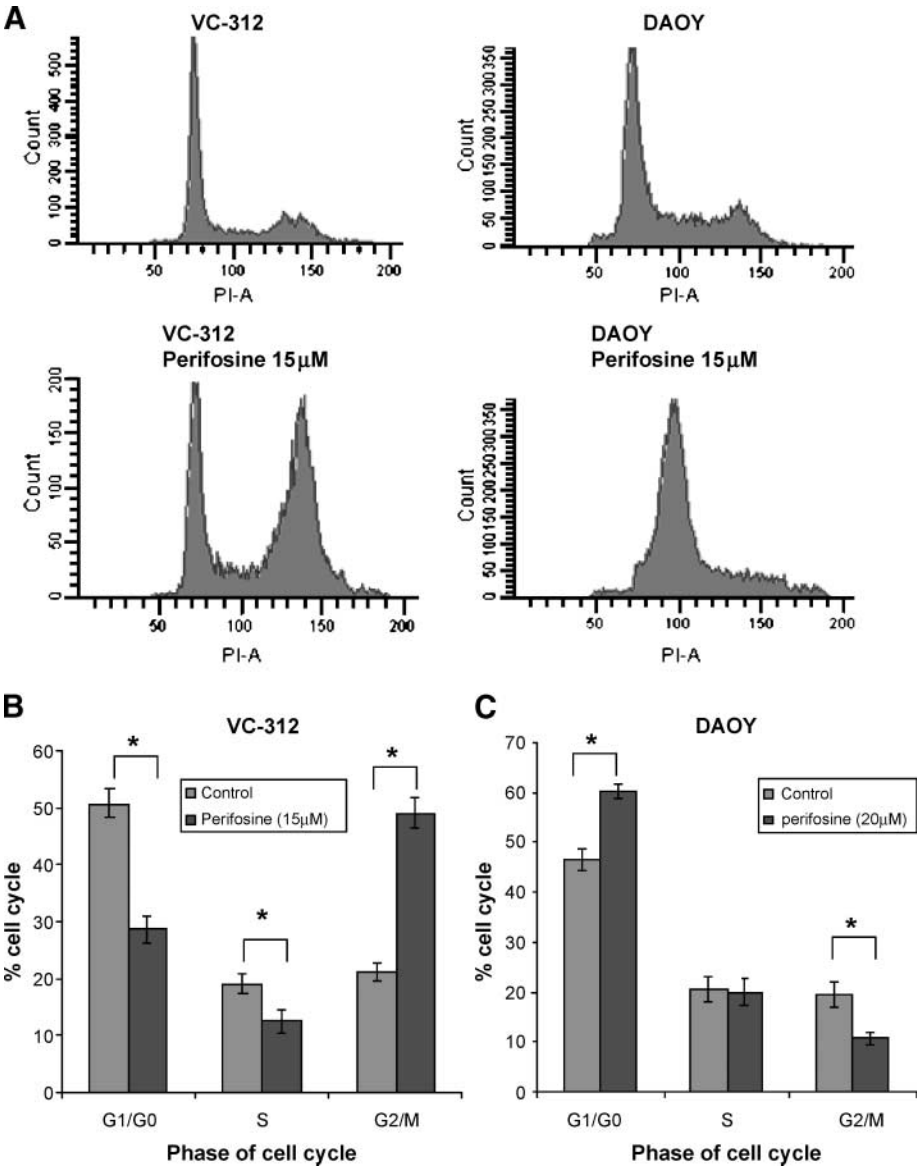

FIGURE 6. Perifosine arrests proliferating medulloblastoma cells at cell cycle checkpoints. Exponentially growing DAOY (**A** and **B**) and VC-312 (**A** and **C**) cells were treated with perifosine (15 μmol/L) and analyzed by flow cytometry. **A.** Representative histograms obtained from flow cytometric analysis of cellular DNA content after staining with propidium iodide (*PI*). **B** and **C.** Analysis of mean percentage of total cells from three independent trials. Means compared with *t* test. Bars, SEM, with significance set at $P = 0.05$. Inset values, relative percentage of cells in G_0/G_1, S, and G_2-M. DNA content was analyzed in medulloblastoma cells treated with 15 μmol/L perifosine for 24 h.

with signal transduction pathways that are critical for cell survival. Due to their distinct mode of action, alkylphospholipid drugs are considered as attractive candidates to combine with chemotherapy and radiotherapy to overcome therapeutic resistance (30). In addition, there is limited efficacy of perifosine monotherapy reported in a variety of solid malignancies. We also tested the effect of perifosine on etoposide and radiation-induced cell death in the two human medulloblastoma cell lines. Perifosine enhanced etoposide and radiation-induced cell death. This effect was additive for VC-312 and synergistic for DAOY, resulting in a marked increase in cell death. Etoposide is a DNA-damaging anticancer drug which targets DNA topoisomerases, interfering with DNA structural modification during DNA synthesis and mitosis, and thereby disabling mitotic progression. Topoisomerase inhibitors have been shown to have inhibitory actions on cell cycle progression in late S and G_2-M phases of the cell cycle (31). This inhibitory mechanism on S phase progression results in late S phase and G_2-M phase arrest, reflective of a DNA repair process in progress, and leading eventually to mitotic catastrophe and cell death (32). In leukemia cells, in addition to G_2-M arrest which results in mitotic cell death, a concurrent induction of apoptosis occurs (33). The observed effects of perifosine on cell cycle arrest in medulloblastoma cells in the present study is similar to that observed in human T-cell leukemias, which show a synergistic cell death effect when cotreated with etoposide (25). The apparent synergy seen in the current study was observed at clinically achievable concentrations of perifosine, which is encouraging for further development of optimal dosing regimens in pediatric patients. Perifosine seems to be a promising adjuvant treatment, deserving of further evaluation in pediatric brain tumors such as medulloblastoma.

Materials and Methods

Cell Culture

Two medulloblastoma cell lines were used in this study, DAOY (from American Type Culture Collection), and VC-312,

Published OnlineFirst November 3, 2009; DOI: 10.1158/1541-7786.MCR-09-0069

established under approved research protocols, and characterized in our laboratory (Pediatric Neuro-Oncology Laboratory, Virginia Commonwealth University). Cells were grown in DMEM supplemented with 10% heat-inactivated fetal bovine serum, glutamine, and 1% penicillin-streptomycin solution at 37°C temperature with 5% CO_2 in a humidified incubator.

Antibodies and Reagents

Antibodies against pan-AKT, phosphorylated AKT (Ser^{473} and Thr^{308}), caspases 3, 7, and 9, and Erk1/2 were purchased from Cell Signaling Technologies. Anti-PARP antibody was obtained from Roche Applied Science. Anti-$p21^{cip1/wafl}$ monoclonal antibody was obtained from DAKO Cytomation. Mouse monoclonal P53 antibody, and phosphorylated Erk1/2 monoclonal antibody were obtained from Santa Cruz Biotechnology, Inc. Perifosine was obtained from Keryx Pharmaceuticals and was reconstituted as a 10 mmol/L stock solution in sterile PBS. Etoposide and cisplatin were purchased from Sigma-Aldrich and reconstituted in DMSO as stock solutions immediately prior to use.

Cell Lysis and Immunoblot Analysis

Cell preparations were subjected to lysis and protein extraction using radioimmunoprecipitation assay lysis buffer (50 mmol/L Tris-HCl, 150 mmol/L NaCl, 1% NP40, 0.5% SDS, and 1% deoxycholic acid) containing protease and phosphatase inhibitors (EMD Biosciences). Cell lysates were collected on ice and centrifuged for 15 min at 14,000 rpm, after shearing with a 1 mL syringe, fitted with a 26-gauge needle. Supernatants were stored at −80°C. Protein concentrations were measured using the DC Protein Assay (Bio-Rad Laboratories). Protein samples were separated by loading 20 or 40 μg of protein on Novex NuPAGE 4% to 12% Bis-Tris gels (Invitrogen), followed by electrophoresis for 55 min, and transferred to nitrocellulose membranes at 35 V for 2 h (Invitrogen). After the transfer was completed, the protein blots were blocked in a buffer solution containing 5% nonfat milk or 5% bovine serum albumin for 1 h at room temperature. The membranes were incubated with primary antibodies overnight at 4°C and then washed four times in TBS containing 0.5% Tween 20. After washing, the membranes were probed with antirabbit or antimouse secondary antibody (1:3,000-1:6,000; Rockland, Inc.) conjugated with horseradish peroxidase for 1.5 h at room temperature. Western blots were developed using the ECL Detection System (GE Healthcare-Amersham Biosciences). β-Actin antibody (1:5,000; Sigma Biotechnology) was used as a control for protein loading.

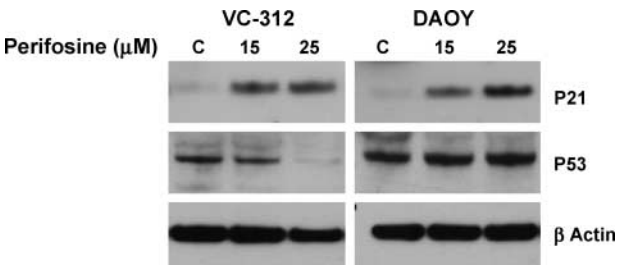

FIGURE 7. Perifosine-induced cell cycle arrest is associated with the induction of p21WAF1. Cell lysates were prepared from DAOY and VC-312 cell lines, exposed to perifosine (15 μmol/L) for 12 h. Western blotting was performed with the antibodies indicated.

Cell Viability Assays

Cell viability was determined using the CellTiter-Glo luminescent ATP assay (Promega, Inc.). Medulloblastoma cells were plated in white, opaque-walled, sterile, 96-well plates at a density of 1,000 cells/100 μL of growth medium per well. Cells were allowed to settle overnight. The next day, cells were treated with the AKT inhibitor perifosine (1-50 μmol/L) versus equimolar solvent control for 24 to 72 h. Viable cells were determined by adding CellTiter-Glo luminescent viability assay lysis reagent (Promega), incubating at room temperature with manual agitation for 2 min then on a rotating platform at 4°C for 10 min, and allowing equilibration for 15 min at room temperature. Luminescence was detected using a luminescent plate reader (Fluostar Optima, BMG Lab Technologies GmbH). Mean relative light units for replicates within each condition were compared using Student's t tests with the significance threshold set at 95% confidence ($P < 0.05$).

Exposure of Cells to Ionizing Radiation

Cells (1×10^6) were plated in a 100-mm dish and left overnight. The next day, cells were irradiated with ^{60}Co γ-rays at a dose rate of 1.1 Gy/min. After 24 h, cells were treated with different concentrations of perifosine. Cell viability was determined after 72 h in cell viability assays as described above.

Cell Cycle Analysis by Flow Cytometry

Cells (1×10^6) were plated in a 100-mm dish, and serum-starved overnight for synchronization. Cells were treated with serum-containing medium after 16 h, with different concentrations of perifosine, and collected after a period of 12 or 24 h. After treatment, cells were trypsinized and cell suspensions washed twice in PBS. Cell fixation was done in 1 mL of 70% ethanol. After 30 min, cells were centrifuged and resuspended in 400 μL of propidium iodide/RNase B solution (Apo-Direct staining solution, BD Biosciences-Pharmingen) for 30 min at room temperature. Cells were measured on a FACScanto flow cytometer and data analyzed using FACSDiva 5.0 software (BD Biosciences).

siRNA Transfection

Cells were transfected with p21 siRNA predesigned validated oligonucleotides, containing sequences directed against p21WAF1 (ABI-Ambion). Cells were plated in six-well plates in triplicate at a density of 2×10^5 cells per well, and allowed to attach overnight. The next day, medium was replaced with 2% serum-containing Optimem. Cells were transfected with siRNA to a final concentration of 25 nmol/L, mixed with OligofectAMINE and 100 μL of Optimem (0% serum) for each well. After transfection, cells were placed on a rocker for 4 h in an incubator at 37°C. After 4 h, cells were supplemented with 1,500 μL of Optimem (10% serum) for 20 h. Twenty-four hours after transfection, cells were treated with 15 μmol/L of perifosine for 24 h. Cells were collected for Western blotting analysis or fixed in 70% ethanol for flow cytometry studies.

Statistical Analysis

Data were evaluated by comparing the means and SEM of replicate experiments. Data are expressed as the mean and SEM of at least three independent experiments. Statistical analysis

Published OnlineFirst November 3, 2009; DOI: 10.1158/1541-7786.MCR-09-0069

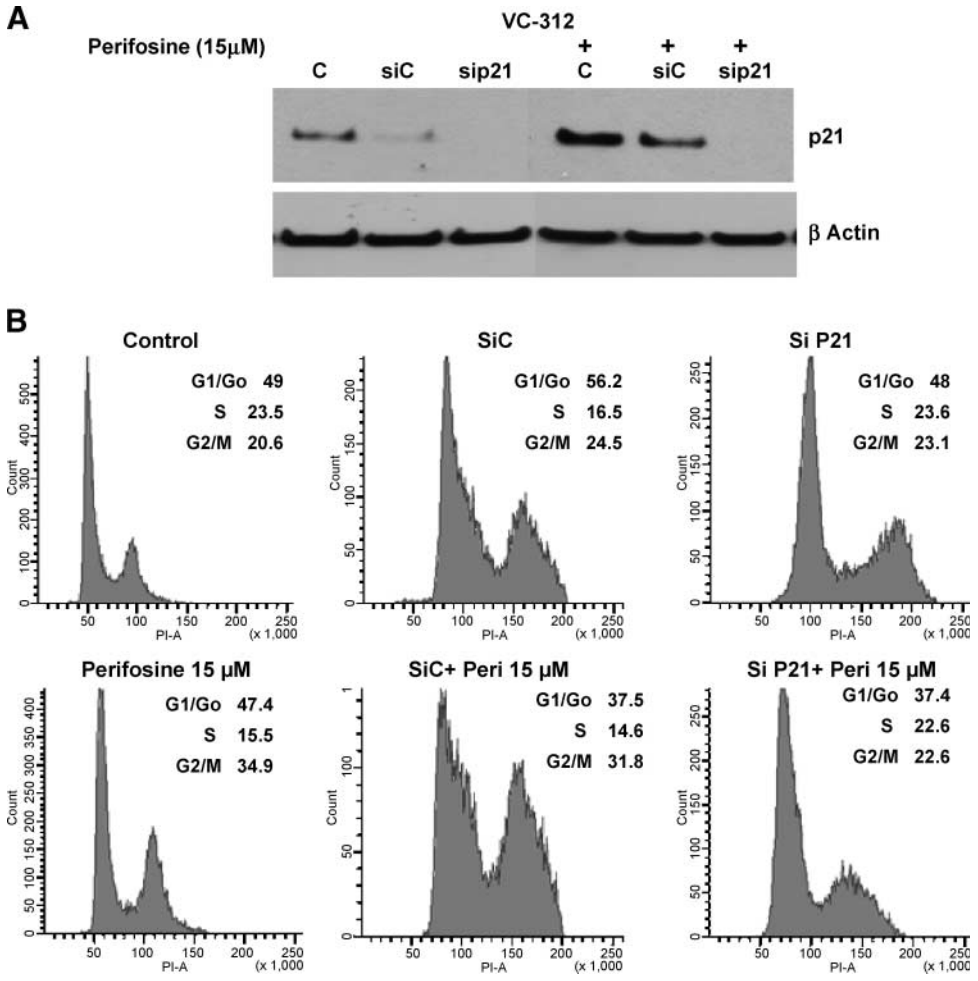

FIGURE 8. Suppression of p21WAF1 by RNA interference reverses perifosine-induced cell cycle arrest in medulloblastoma. **A.** Suppression of p21 protein expression is observed by Western blotting 48 h after transfection. **B.** Cell cycle analysis of p21WAF1 siRNA and control treated medulloblastoma cells in the presence or absence of perifosine (15 μmol/L).

was done using an unpaired Student's t test. $P < 0.05$ was considered significant.

Disclosure of Potential Conflicts of Interest

No potential conflicts of interest were disclosed.

References

1. Sarkar C, Deb P, Sharma MC. Recent advances in embryonal tumours of the central nervous system. Childs Nerv Syst 2005;4:272–93.

2. Ribi K, Relly C, Landolt MA, Alber FD, Boltshauser E, Grotzer MA. Outcome of medulloblastoma in children: long-term complications and quality of life. Neuropediatrics 2005;36:357–65.

3. Raffel C, Jenkins RB, Frederick L, et al. Sporadic medulloblastomas contain PTCH mutations. Cancer Res 1997;57:842–5.

4. Gilbertson RJ. Medulloblastoma: signalling a change in treatment. Lancet Oncol 2004;5:209–18.

5. Staal SP, Hartley JW, Rowe WP. Isolation of transforming murine leukemia viruses from mice with a high incidence of spontaneous lymphoma. Proc Natl Acad Sci U S A 1977;74:3065–7.

6. Wlodarski P, Grajkowska W, £ojek M, Rainko K, JóŸwiak J. Activation of Akt and Erk pathways in medulloblastoma. Folia Neuropathol 2006;44:214–20.

7. Bellacosa A, Kumar CC, Di Cristofano A, Testa JR. Activation of AKT kinases in cancer: implications for therapeutic targeting. Adv Cancer Res 2005;94:29–86.

8. Vanhaesebroeck B, Alessi DR. The PI3K-PDK1 connection: more than just a road to PKB. Biochem J 2000;3:561–76.

9. Rao G, Pedone CA, Valle LD, Reiss K, Holland EC, Fults DW. Sonic hedgehog and insulin-like growth factor signaling synergize to induce medulloblastoma formation from nestin-expressing neural progenitors in mice. Oncogene 2004;23:6156–62.

10. Cheng JQ, Lindsley CW, Cheng GZ, Yang H, Nicosia SV. The Akt/PKB pathway: molecular target for cancer drug discovery. Oncogene 2005;24:7482–792.

11. Crul M, Rosing H, de Klerk GJ, et al. Phase I and pharmacological study of daily oral administration of perifosine (D-21266) in patients with advanced solid tumours. Eur J Cancer 2002;38:1615–21.

12. Leighl NB, Dent S, Clemons M, et al. A Phase 2 study of perifosine in advanced or metastatic breast cancer. Breast Cancer Res Treat 2008;108:87–92.

13. Papa V, Tazzari PL, Chiarini F, et al. Proapoptotic activity and chemosensitizing effect of the novel Akt inhibitor perifosine in acute myelogenous leukemia cells. Leukemia 2008;22:147–60.

14. Ruiter GA, Zerp SF, Bartelink H, van Blitterswijk WJ, Verheij M. Anti-cancer alkyl-lysophospholipids inhibit the phosphatidylinositol 3-kinase-Akt/PKB survival pathway. Anticancer Drugs 2003;14:167–73.

15. Vink SR, Schellens JH, van Blitterswijk WJ, Verheij M. Tumor and normal tissue pharmacokinetics of perifosine, an oral anti-cancer alkylphospholipid. Invest New Drugs 2005;23:279–86.

16. Kondapaka SB, Singh SS, Dasmahapatra GP, Sausville EA, Roy KK. Perifosine, a novel alkylphospholipid, inhibits protein kinase B activation. Mol Cancer Ther 2003;2:1093–103.

17. Li X, Luwor R, Lu Y, Liang K, Fan Z. Enhancement of antitumor activity of

Published OnlineFirst November 3, 2009; DOI: 10.1158/1541-7786.MCR-09-0069

the anti-EGF receptor monoclonal antibody cetuximab/C225 by perifosine in PTEN-deficient cancer cells. Oncogene 2006;25:525–35.

18. Patel V, Lahusen T, Sy T, Sausville EA, Gutkind JS, Senderowicz AM. Perifosine, a novel alkylphospholipid, induces p21(WAF1) expression in squamous carcinoma cells through a p53-independent pathway, leading to loss in cyclin-dependent kinase activity and cell cycle arrest. Cancer Res 2002;62:1401–9.

19. Floryk D, Thompson TC. Perifosine induces differentiation and cell death in prostate cancer cells. Cancer Lett 2008;266:216–26.

20. Vivanco I, Sawyers CL. The phosphatidylinositol 3-kinase AKT pathway in human cancer. Nat Rev Cancer 2002;2:489–501.

21. Hartmann W, Digon-Söntgerath B, Koch A, et al. Phosphatidylinositol 3′-kinase/AKT signaling is activated in medulloblastoma cell proliferation and is associated with reduced expression of PTEN. Clin Cancer Res 2006;12:3019–27.

22. Steelman LS, Bertrand FE, McCubrey JA. The complexity of PTEN: mutation, marker and potential target for therapeutic intervention. Expert Opin Ther Targets 2004;8:537–50.

23. Ruggeri BA, Huang L, Wood M, Cheng JQ, Testa JR. Amplification and overexpression of the AKT2 oncogene in a subset of human pancreatic ductal adenocarcinomas. Mol Carcinog 1998;21:81–6.

24. van der Luit AH, Budde M, Ruurs P, Verheij M, van Blitterswijk WJ. Alkyl-lysophospholipid accumulates in lipid rafts and induces apoptosis via raft-dependent endocytosis and inhibition of phosphatidylcholine synthesis. J Biol Chem 2002;277:39541–7.

25. Nyåkern M, Cappellini A, Mantovani I, Martelli AM. Synergistic induction of apoptosis in human leukemia T cells by the Akt inhibitor perifosine and etoposide through activation of intrinsic and Fas-mediated extrinsic cell death pathways. Mol Cancer Ther 2006;5:1559–70.

26. Steelman LS, Pohnert SC, Shelton JG, Franklin RA, Bertrand FE, McCubrey JA. JAK/STAT, Raf/MEK/ERK, PI3K/Akt and BCR-ABL in cell cycle progression and leukemogenesis. Leukemia 2004;18:189–218.

27. Gajate C, Mollinedo F. Edelfosine and perifosine induce selective apoptosis in multiple myeloma by recruitment of death receptors and downstream signaling molecules into lipid rafts. Blood 2007;109:711–9.

28. Gross A. BID as a double agent in cell life and death. Cell Cycle 2006;5:582–4.

29. Sherr CJ, Roberts JM. CDK inhibitors: positive and negative regulators of G1-phase progression. Genes Dev 1999;13:1501–12.

30. Vink SR, van Blitterswijk WJ, Schellens JH, Verheij M. Rationale and clinical application of alkylphospholipid analogues in combination with radiotherapy. Cancer Treat Rev 2007;33:191–202.

31. Sugimoto K, Tamayose K, Takagi M, et al. Activation of an ataxia telangiectasia mutation-dependent intra-S-phase checkpoint by anti-tumour drugs in HL-60 and human lymphoblastoid cells. Br J Haematol 2000;110:819–25.

32. Elrod HA, Lin YD, Yue P, et al. The alkylphospholipid perifosine induces apoptosis of human lung cancer cells requiring inhibition of Akt and activation of the extrinsic apoptotic pathway. Mol Cancer Ther 2007;6:2029–38.

33. Rahmani M, Reese E, Dai Y, et al. Coadministration of histone deacetylase inhibitors and perifosine synergistically induces apoptosis in human leukemia cells through Akt and ERK1/2 inactivation and the generation of ceramide and reactive oxygen species. Cancer Res 2005;65:2422–32.

AACR American Association for Cancer Research

Molecular Cancer Research

The Alkylphospholipid Perifosine Induces Apoptosis and p21-Mediated Cell Cycle Arrest in Medulloblastoma

Anil Kumar, Helen L. Fillmore, Renu Kadian, et al.

Mol Cancer Res 2009;7:1813-1821. Published OnlineFirst November 3, 2009.